11832 *Inorg. Chem.* **2009**, *48*, 11832–11842
DOI: 10.1021/ic901880f

Inorganic Chemistry
Article

Highly Fluorous Complexes of Ruthenium and Osmium and Their Solubility in Supercritical Carbon Dioxide

Bradley M. Berven,[†] George A. Koutsantonis,*[,†] Brian W. Skelton,[†] Robert D. Trengove,[‡] and Allan H. White[†]

[†]*Chemistry, School of Biomedical, Biomolecular and Chemical Sciences, University of Western Australia, 35 Stirling Highway, Crawley, WA, Australia, 6009 and* [‡]*School of Biological Sciences and Biotechnology and School of Pharmacy, Murdoch University, Murdoch, Western Australia, 6150*

Received September 23, 2009

A series of ruthenium and osmium complexes containing highly fluorous diphosphine ligands $^{F}P\hat{}P^{F}$ = $(F_{13}C_6C_6H_4\text{-}p)_2P(CH_2)_2P(p\text{-}C_6H_4C_6F_{13})_2$ (dfppe) and $(F_{13}C_6C_6H_4\text{-}p)_2P(CH_2)_3P(p\text{-}C_6H_4C_6F_{13})_2$ (dfppp) has been prepared. The fluorous diphosphine ligands incorporate four C_6F_{13} "fluoro-ponytails", and these have been effective in solubilizing the complexes in supercritical carbon dioxide ($scCO_2$). Precise solubility measurements in $scCO_2$ were performed for some of the complexes. The new complexes $[MX_2(^{F}P\hat{}P^{F})_2]$ and $[MX(^{F}P\hat{}P^{F})(\eta\text{-}C_5H_5)]$, M = Ru, Os, X = Cl, Br, have been characterized by a number of spectroscopic techniques and their electrochemical properties measured, three of the ruthenium complexes also being characterized by single-crystal X-ray studies. The noncovalent interactions observed in the X-ray structures have been analyzed by the Hirshfeld surface approach, putting them on a more solid footing. The fluorinated complexes show significantly different solvation properties from those of the analogous unfluorinated compounds, particularly with respect to their behavior in common organic solvents and their good $scCO_2$ solubility.

Introduction

The extensive diversity of ligands available for the formation of metal complexes and the variations in their steric and electronic characteristics gives the synthetic chemist the ability to fine-tune the desired properties of a transition metal complex through a judicious choice of the coordinated ligand.[1] Metal complexes with an unusually high charge or high oxidation state can be better stabilized by an appropriate choice of ligand. The solubility and phase-transfer behavior of metal complexes is also affected by the choice of ligand, with these physical properties being important factors in chemical reactions that employ metal-based catalysts or phase-transfer agents. In particular, as the chemical industry moves away from environmentally impacting solvents, less objectionable alternatives such as supercritical carbon dioxide ($scCO_2$) become attractive vehicles for nonpolar or weakly polar chemical reactions.[2−4] These "greener" solvents are often more than just a medium in which to conduct the reaction; they are also able to participate in the course of the chemical reaction in which they are employed, with the consequences perceived as beneficial or otherwise. Thus, the solubilization of metal complexes in these supercritical fluids (SCFs) is often dependent upon an appropriate configuration of the ligand array. In particular, the fluorination of substituent groups can lead to a marked improvement in the $scCO_2$ solubility,[5] with many fluorous complexes being employed for catalysis in $scCO_2$.[6−9] Moreover, in the field of fluorous biphasic catalysis, the attachment of a single perfluorinated group to a phosphine in some rhodium complexes can be sufficient to partition them into perfluoromethylcyclohexane, in preference to toluene,[5] with such examples offering the chemical industry the possibility of recycling homogeneous catalysts.

The chemistry of ruthenium(II) complexes that contain tertiary phosphines has been widely investigated, particularly in connection with their homogeneous catalytic activity for a variety of reactions.[10,11] Since their discovery,[12] complexes

*To whom correspondence should be addressed. Fax: (+61) 8 6488 7247. E-mail: george.koutsantonis@uwa.edu.au.

(1) Reek, J. N. H.; Sandee, A. J. *Dalton Trans.* **2006**, 3385.
(2) Kendall, J. L.; Canelas, D. A.; Young, J. L.; DeSimone, J. M. *Chem. Rev.* **1999**, *99*, 543–563.
(3) Jessop, P. G.; Leitner, W. *Chemical Synthesis Using Supercritical Fluids*; Wiley-VCH: Weinheim, Germany,1999.
(4) Blanchard, L. A.; Hancu, D.; Beckman, E. J.; Brennecke, J. F. *Nature* **1999**, *399*, 28–29.
(5) Gladysz, J. A.; Corrêa da Costa, R. *Handbook of Fluorous Chemistry*; Wiley-VCH: Weinheim, Germany, 2004; pp 24−40.
(6) DeSimone, J. M.; Tumas, W. *Green Chemistry Using Liquid and Supercritical Carbon Dioxide*; Oxford University Press: New York, 2003.
(7) Francio, G.; Wittmann, K.; Leitner, W. *J. Organomet. Chem.* **2001**, *621*, 130.
(8) He, L.-N.; Choi, J.-C.; Sakakura, T. *Tetrahedron Lett.* **2001**, *42*, 2169.
(9) Jessop, P. G.; Hsiao, Y.; Ikariya, T.; Noyori, R. *J. Am. Chem. Soc.* **1994**, *116*, 8851–8852.
(10) Trost, B. M.; Frederiksen, M. U.; Rudd, M. T. *Angew. Chem., Int. Ed.* **2005**, *44*, 6630.
(11) Murahashi, S.-I. *Ruthenium in Organic Synthesis*; Wiley-VCH: Weinheim, Germany, 2004.
(12) Chatt, J.; Hayter, R. G. *J. Chem. Soc.* **1961**, 896.

 Published on Web 11/25/2009

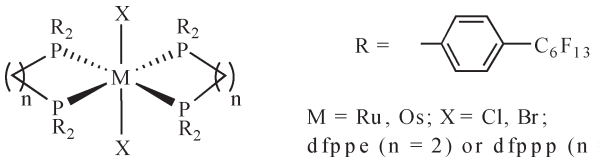

Figure 1. Schematic of the *trans*-[MX_2 (fluorous-diphosphine)$_2$] complexes.

with chelating diphosphines of the type *cis*- or *trans*-[$RuCl_2$(diphosphine)$_2$] have enjoyed persistent interest. They are readily made from many precursors including $RuCl_3 \cdot xH_2O$,[12] [$RuCl_2(DMSO)_4$],[13,14] $K_2[RuCl_5(H_2O)]$,[15] and [$RuCl_2(PPh_3)_3$].[16,17] The osmium(II) analogs [OsX_2(diphosphine)$_2$], X = Cl, Br, are also readily accessible from precursors which include $(NH_4)_2[OsX_6]$, X = Cl,[18] Br;[19] $[X_4Os{\equiv}OsX_4]^{2-}$, X = Cl, Br;[20] and [$OsCl_2(DMSO)_4$].[21] This paper describes simple procedures for the synthesis of these [$MX_2(^FP\text{^}P^F)_2$] complexes, M = Ru, Os; X = Cl, Br; $P^F{}_2$ = dfppe, $(F_{13}C_6C_6H_4\text{-}p)_2P(CH_2)_2P(p\text{-}C_6H_4C_6F_{13})_2$, and dfppp, $(F_{13}C_6C_6H_4\text{-}p)_2P(CH_2)_3P(p\text{-}C_6H_4C_6F_{13})_2$ (Figure 1). It should be noted that the synthesis of the ligands, on the other hand, was somewhat challenging, and it appears elsewhere.[22]

Very few metal complexes have had their $scCO_2$ solubility measured,[23] and even fewer fluorous−phosphine metal complexes have had this property measured.[24−26] This is somewhat surprising given that numerous fluorous complexes have been applied as catalysts in $scCO_2$, and the solubility of a catalyst in the solvent for the reaction is of fundamental importance. Thus, we undertook the measurement of the $scCO_2$ solubility of the [$MX_2(^FP\text{^}P^F)_2$] complexes. These compounds contain eight C_6F_{13} tails, and for comparative purposes, the complexes [$MX(^FP\text{^}P^F)(\eta\text{-}C_5H_5)$], M = Ru, Os; X = Cl, Br, $P^F{}_2$ = dfppe, dfppp, containing four C_6F_{13} tails, have also been prepared and their $scCO_2$ solubility measured. Our method for the solubility measurement has been tested against other known methods, giving reliable solubility data,[27] and this will be elaborated on in the Results and Discussion.

Several ruthenium complexes of the type *cis*- or *trans*-[$RuCl_2P_4$], where P = PMe_3 or P_2 = dppe, have shown excellent catalytic activity for reactions employing $scCO_2$ as a solvent and reactant (e.g., Scheme 1).[28] The turnover number for dimethylformamide (DMF) production is very high,[28] one reason being the excellent miscibility of hydrogen in the supercritical fluid. Chemistry of this type also offers the attractive prospect of CO_2 fixation, which provides the impetus for this work. The parent complex, [$RuCl_2$(dppe)$_2$], itself is not soluble in $scCO_2$,[29] but it is solubilized in the dimethylammonium dimethylcarbamate phase formed in the reaction. Thus, it is still an active catalyst for DMF production. However, the incorporation of eight C_6F_{13} "tails" in [$RuCl_2$(dfppe)$_2$] should impart good solubility in $scCO_2$ (seen later), and therefore potentially higher catalytic activity in the fluid.

Scheme 1. Production of DMF in $scCO_2$ with [$RuCl_2P_4$] Type Catalysts

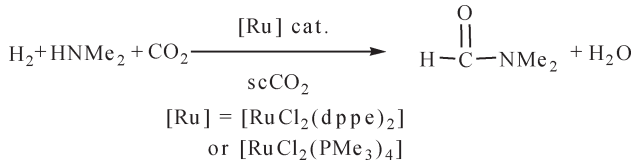

Experimental Section

Manipulations of oxygen- and moisture-sensitive materials were carried out under an atmosphere of high-purity argon using standard Schlenk techniques, or in a drybox (Miller Howe) equipped with H_2O (molecular sieves), O_2 (CuO), and solvent (activated charcoal) removal columns.

^1H, ^{13}C, and ^{31}P NMR spectra were acquired using a Varian Gemini 200 (^1H at 200 MHz and ^{13}C at 50.3 MHz), Bruker AM 300 (^1H at 300 MHz and ^{13}C at 75.5 MHz), or Bruker ARX 500 (^1H at 500 MHz, ^{13}C at 125.8 MHz, and ^{31}P at 202.5 MHz) instruments. NMR spectra were internally referenced. ^1H chemical shifts were referenced to incompletely deuterated solvent signals; ^{13}C chemical shifts were referenced to the deuterated solvents. ^{31}P NMR spectra were referenced externally to 85% H_3PO_4. Chemical shifts (δ) are in parts per million (ppm) and quoted coupling constants (J) are given in Hertz.

Mass spectra were recorded on a VG AutoSpec spectrometer operating with an 8 kV accelerating voltage in the FAB^+ (fast atom bombardment—positive ion, using nitrobenzyl alcohol as the matrix) or ESI^+ (electrospray ionization—positive ion) modes.

Cyclic voltammograms were recorded using a MacLab Potentiosat controlled by an Apple Macintosh LC computer equipped with the AD Instruments Echem software (v. 1.5.1). A platinum working electrode (flat disk), a platinum counter-electrode, and a silver/silver chloride reference electrode were used. All solutions were 1−5 mmol L^{-1} of analyte in a 0.1 M [(^{t}Bu)$_4$N][ClO_4] solution in CH_2Cl_2. Dichloromethane was purified by distillation from calcium hydride under argon and stored under argon. All solutions were prepurged with high-purity argon for 20 min and measurement made under a flow of argon at ambient temperatures.

Solvent distillations were conducted under an atmosphere of dry high-purity argon. Tetrahydrofuran (HPLC-grade) was predried over sodium wire and distilled from potassium benzophenone ketyl. Hexane was distilled from sodium/potassium alloy (NaK), while diethyl ether, toluene, and

(13) Bautista, M. T.; Cappellani, E. P.; Drouin, S. D.; Morris, R. H.; Schweitzer, C. T.; Sella, A.; Zubkowski, J. *J. Am. Chem. Soc.* **1991**, *113*, 4876.
(14) Winter, R. F.; Brunner, B. M.; Scheiring, T. *Inorg. Chim. Acta* **2000**, *310*, 21.
(15) Bressan, M.; Rigo, P. *Inorg. Chem.* **1975**, *14*, 2286.
(16) Jung, C. W.; Garrou, P. E.; Hoffman, P. R.; Caulton, K. G. *Inorg. Chem.* **1984**, *23*, 726.
(17) Mason, R.; Meek, D. W.; Scollary, G. R. *Inorg. Chim. Acta* **1976**, *16*, L11.
(18) Sullivan, B. P.; Meyer, T. J. *Inorg. Chem.* **1982**, *21*, 1037.
(19) Maltby, P. A.; Schlaf, M.; Steinbeck, M.; Lough, A. J.; Morris, R. H.; Klooster, W. T.; Koetzle, T. F.; Srivastava, R. C. *J. Am. Chem. Soc.* **1996**, *118*, 5396.
(20) Fanwick, P. E.; Fraser, I. F.; Tetrick, S. M.; Walton, R. A. *Inorg. Chem.* **1987**, *26*, 3786.
(21) McDonagh, A. M.; Humphrey, M. G.; Hockless, D. C. R. *Tetrahedron: Asymmetry* **1997**, *8*, 3579.
(22) Berven, B. M.; Koutsantonis, G. A. *Synthesis* **2008**, 2626.
(23) Smart, N. G.; Carleson, T.; Kast, T.; Clifford, A. A.; Burford, M. D.; Wai, C. M. *Talanta* **1997**, *44*, 137–150.
(24) Dahmen, N.; Griesheimer, P.; Makarczyk, P.; Pitter, S.; Walter, O. *J. Organomet. Chem.* **2005**, *690*, 1467.
(25) Stibrany, R. T.; Gorun, S. M. *J. Organomet. Chem.* **1999**, *579*, 217.
(26) Kainz, S.; Koch, D.; Baumann, W.; Leitner, W. *Angew. Chem., Int. Ed. Engl.* **1997**, *36*, 1628–1630.
(27) Graham, B. F. Ph.D. Thesis, University of Western Australia, Crawley, WA, Australia, **2000**.
(28) Jessop, P. G.; Hsiao, Y.; Ikariya, T.; Noyori, R. *J. Am. Chem. Soc.* **1996**, *118*, 344.
(29) Ikariya, T.; Noyori, R. *Green Chemistry Using Liquid and Supercritical Carbon Dioxide*; Oxford University Press: Oxford, U. K., 2003; pp 56−57.

xylenes were distilled from sodium. Dichloromethane (AR-grade) was distilled from calcium hydride. DMSO (AR-grade) was distilled under reduced pressure and stored over 4 Å molecular sieves.

Supercritical carbon dioxide extraction experiments were conducted using a Hewlett-Packard 7680T Supercritical Fluid Extraction (SFE) Module. Carbon dioxide used for solubility measurements was grade N45, high purity, from Air Liquide. The following procedure was used: A sample was loaded into a stainless steel thimble, which was then pressurized with $scCO_2$. The SCF remained in the thimble for a given equilibration (dissolution) time, followed by transfer of this solution and its depressurization onto a trap containing a stationary phase. The trap was a small column of octadecyl silica (ODS), which was then washed with an organic solvent to remove the dissolved compound into glass vials. When the solvent had evaporated, the tared vials were weighed and the mass of the $scCO_2$-dissolved compound determined. The total error associated with this mass determination, which was conducted on a four-point balance, was estimated to be ±0.5 mg. The mass loss for the thimble after extraction was also determined and generally agreed with the mass of the sample washed through to the vials. The total error associated with this mass loss determination, which was conducted on a four-point balance, was estimated to be ±0.1 mg (no buoyancy correction). Each solubility measurement was conducted in triplicate, and for those compounds that exhibited the highest $scCO_2$ solubility, the maximum relative standard deviation was 1.3%. For those compounds that exhibited the lowest $scCO_2$ solubility, the maximum relative standard deviation was 15.4%.

$[RuCl_2(DMSO)_4]$,[30] $[RuCl(PPh_3)_2(\eta\text{-}C_5H_5)]$,[31] $[OsBr(PPh_3)_2(\eta\text{-}C_5H_5)]$,[32] and $[OsCl_2(PPh_3)_3]$[33] were prepared by published procedures; $[OsBr_2(PPh_3)_3]$ was prepared from $(NH_4)_2[OsBr_6]$ using a procedure analogous to that of the chloride complex. The fluorous diphosphines were prepared as reported.[22]

Synthesis of *trans*-[$RuCl_2$(dfppp)$_2$] (1). To a suspension of $[RuCl_2(DMSO)_4]$ (0.19 g, 0.39 mmol) in toluene (5 mL) was added a 45 °C solution of dfppp (1.32 g, 0.78 mmol) in toluene (30 mL), with stirring. The mixture was heated to 60 °C for 24 h, after which it was cooled to room temperature. This afforded an orange precipitate, which was filtered in the air and washed with *n*-hexane (30 mL) to yield **1** as a pale orange powder (1.12 g, 0.32 mmol, 82%). It should be noted that solutions of the complex slowly decompose when handled aerobically, although the solid was air-stable. ^{1}H NMR ($CDCl_3$): δ 7.44 (br m, 16H, Ar−H), δ 7.29 (m, 16H, Ar−H), δ 2.69 (br m, 8H, PCH_2), 1.90 (br m, 4H, CH_2). $^{31}P\{^1H\}$ NMR ($CDCl_3$): δ −2.1 (s). $^{13}C\{^1H\}$ NMR ($CDCl_3$): δ 134.8 (m, C_{ortho}), δ 130.9 (d, $^1J_{C-P}$ = 10 Hz, C_{ipso}), δ 130.5 (t, $^2J_{C-F}$ = 25 Hz, C_{para}), δ 125.7 (m, C_{meta}), δ 121−108 (overlapping m, C_6F_{13} tail), δ 27.5 (m, PCH_2), δ 19.2 (m, CH_2). Melting point = 183−185 °C. Anal. Calcd for $C_{102}H_{44}Cl_2F_{104}P_4Ru$: C, 34.60; H, 1.25. Found: C, 34.72; H, 1.31. Single crystals for the X-ray structure determination were obtained by slow evaporation of a $CHCl_3$ solution of the compound.

Synthesis of *trans*-[$RuCl_2$(dfppe)$_2$] (2). A mixture of dfppe (200 mg, 0.12 mmol), $[RuCl_2(DMSO)_4]$ (29 mg, 0.06 mmol), and toluene (30 mL) was heated at 80 °C for 24 h. The reaction mixture was cooled to 0 °C, which deposited a yellow oil. This oil was dissolved by the addition of Et_2O (20 mL) and moderate warming of the solution. The volume was then reduced by half, followed by cooling to 0 °C, affording a yellow precipitate. Subsequent heating to 55 °C and then slow cooling of the solution to room temperature overnight gave yellow crystals of **2** (120 mg, 0.034 mmol, 57%). By $^{31}P\{^1H\}$ NMR, this was a 3:1 mixture of *cis*- and *trans*-**2** (δ $^{31}P_{cis}$ = 62 and 49 ppm; δ $^{31}P_{trans}$ = 52 ppm). This mixture was then recrystallized from Et_2O/hexane, affording pure *cis*-**2** as a yellow powder (10 mg, 2.8 μmol, 4.7%). ^{1}H NMR (d_6-acetone): δ 8.7−6.8 (m, 32H, Ar−H), δ 3.2 (br m, 8H, CH_2CH_2). $^{31}P\{^1H\}$ NMR (d_6-acetone): δ 61.9 (m, P *trans* to Cl), δ 48.9 (m, P *trans* to P). MS (FAB^+): 3513 $[M]^+$, 3476 $[M - Cl]^+$. Anal. Calcd for $C_{100}H_{40}Cl_2F_{104}P_4Ru$: C, 34.19; H, 1.15. Found: C, 34.78; H, 1.41.

Synthesis of *trans*-[$OsBr_2$(dfppp)$_2$] (3). A solution of $[OsBr_2(PPh_3)_3]$ (0.15 g, 0.13 mmol) in toluene (30 mL) was added to a solution of dfppp (0.5 g, 0.3 mmol) in toluene/Et_2O (80/20, 50 mL total). This was stirred under argon for 1 h at room temperature. The stirring was ceased, and the flask was left standing for 12 h, affording golden-tan crystals of **3** (0.2 g, 0.054 mmol, 41%), which were filtered aerobically, washed with *n*-hexane (20 mL), and dried in vacuo. ^{1}H NMR (d_6-acetone): δ 7.7−7.3 (m, 32H, Ar−H), δ 3.2−3.1 (m, 8H, PCH_2), δ 2.0 (m, 4H, CH_2). $^{31}P\{^1H\}$ NMR (diethyl ether, unlocked): δ −55.0 (s). Anal. Calcd for $C_{102}H_{44}Br_2F_{104}OsP_4$: C, 32.94; H, 1.19. Found: C, 32.82; H, 1.24.

Synthesis of *trans*-[$OsCl_2$(dfppp)$_2$] (4). A solution of $[OsCl_2(PPh_3)_3]$ (45 mg, 0.043 mmol) in toluene (20 mL) was added to a solution of dfppp (150 mg, 0.09 mmol) in toluene/Et_2O (80/20, 11.5 mL total). The mixture was stirred under argon at room temperature for 5 h, at which point the reaction was complete by thin layer chromatography (TLC). After standing under argon for 12 h, the reaction mixture was filtered aerobically, affording complex **4** as a pale green powder, dried in vacuo (75 mg, 0.021 mmol, 49%). ^{1}H NMR (d_6-acetone): δ 7.8−7.3 (m, 32H, Ar−H), δ 3.1−2.9 (br m, 8H, PCH_2), δ 2.0 (m, 4H, CH_2). $^{31}P\{^1H\}$ NMR (d_6-acetone): δ −47.5 (s). $^{13}C\{^1H\}$ NMR (d_6-acetone): δ 136.4 (m, C_{ortho}), δ 130.2 (m, C_{ipso} and C_{para}), δ 126.4 (m, C_{meta}), δ 120−108 (overlapping m, C_6F_{13} tail), δ 26.7 (m, PCH_2), δ 19.9 (m, CH_2). MS (FAB^+): 3632 $[M]^+$. Anal. Calcd for $C_{102}H_{44}Cl_2F_{104}OsP_4$: C, 33.75; H, 1.22. Found: C, 34.00; H, 1.31.

Synthesis of [RuCl(dfppp)(η-C_5H_5)] (5). A mixture of $[RuCl(PPh_3)_2(\eta\text{-}C_5H_5)]$ (44 mg, 0.06 mmol), dfppp (100 mg, 0.06 mmol), and toluene (20 mL) was refluxed under argon for 2 days. The solvent was then removed on a rotary evaporator, leaving a yellow-orange residue. This was dissolved in Et_2O, and after preparative TLC on silica (15% acetone/85% hexane), complex **5** was isolated as a yellow/brown solid (77 mg, 0.041 mmol, 68%). ^{1}H NMR ($CDCl_3$): δ 7.8−7.3 (m, 16H, Ar−H), δ 4.5 (s, 5H, C_5H_5), δ 3.0 (m, 2H, PCH_2), δ 2.5 (m, 1H, PCH_2-$CHHCH_2P'$), δ 2.4 (m, 2H, $P'CH_2$), δ 1.5 (m, 1H, PCH_2CH-HCH_2P'). $^{31}P\{^1H\}$ ($CDCl_3$): δ 40.8 (s). $^{13}C\{^1H\}$ NMR ($CDCl_3$): δ 144.4 (at, J = 20 Hz, C_{ipso}), δ 142.3 (at, J = 21 Hz, C'_{ipso}), δ 133.3 (at, C_{ortho}), δ 132.4 (at, C'_{ortho}), δ 130.7 (t, $^2J_{C-F}$ = 25 Hz, C_{para}), δ 130.1 (t, $^2J_{C-F}$ = 25 Hz, C'_{para}), δ 126.8 (m, C_{meta}), δ 120−108 (overlapping m, C_6F_{13} tails), δ 81.2 (s, Cp), δ 24.0 (vt, J_{C-P} = 15 Hz, PCH_2), δ 21.4 (s, CH_2). Melting point = 68−71 °C. MS (ESI^+) 1886 $[M]^+$, 1851 $[M - Cl]^+$. Anal. Calcd. for $C_{56}H_{27}ClF_{52}P_2Ru$: C, 35.66; H, 1.44. Found: C, 35.74; H, 1.53. Single crystals for the X-ray structure determination were obtained by diffusion of *n*-pentane into a $CHCl_3$ solution of the compound at 5 °C.

Synthesis of [RuCl(dfppe)(η-C_5H_5)] (6). A mixture of $[RuCl(PPh_3)_2(\eta\text{-}C_5H_5)]$ (65 mg, 0.09 mmol) and dfppe (160 mg, 0.10 mmol) was heated at reflux in toluene (30 mL) for 4 h. The solvent was then removed in vacuo, leaving a yellow residue. To this was added CH_2Cl_2 and hexane, followed by volume reduction until a precipitate began to form. The flask was then cooled to −25 °C for 12 h. The yellow precipitate was filtered and washed with cold cyclohexane, affording compound **6** as a

(30) Evans, I. P.; Spencer, A.; Wilkinson, G. *J. Chem. Soc., Dalton Trans.* **1973**, 204.
(31) Bruce, M. I.; Windsor, N. J. *Aust. J. Chem.* **1977**, *30*, 1601.
(32) Bruce, M. I.; Low, P. J.; Skelton, B. W.; Tiekink, E. R. T.; Werth, A.; White, A. H. *Aust. J. Chem.* **1995**, *48*, 1887.
(33) Elliot, G. P.; Mcauley, N. M.; Roper, W. R. *Inorg. Synth.* **1989**, *26*, 184.

yellow powder, dried in vacuo (111 mg, 0.059 mmol, 66%). ^{1}H NMR (CD_2Cl_2): δ 8.1−7.3 (m, 16H, Ar−H), δ 4.6 (s, 5H, C_5H_5), δ 2.8 (m, 2H, CH_2), δ 2.6 (m, 2H, CH_2). ^{31}P{^{1}H} NMR (CD_2Cl_2): δ 82.1 (s). ^{13}C{^{1}H} NMR ($CDCl_3$): δ 144.6 (m, C_{ipso}), δ 138.0 (m, C'_{ipso}), δ 134.0 (m, C_{ortho}), δ 131.3 (m, C'_{ortho}), δ 130.5 (m, C_{para}), δ 130.1 (t, $^2J_{C-F}$ = 25 Hz, C'_{para}), δ 126.9 (m, C_{meta}), δ 120−106 (overlapping m, C_6F_{13} tails), δ 81.0 (s, Cp), δ 27.2 (t, J_{C-P} = 22 Hz, CH_2). Melting point = 78−80 °C. MS (FAB$^+$): 1871 [M]$^+$, 1836 [M − Cl]$^+$. Anal. Calcd. for $C_{55}H_{25}ClF_{52}P_2Ru$: C, 35.28; H, 1.35. Found: C, 35.45; H, 1.46.

Synthesis of [OsBr(dfppp)(η-C_5H_5)] (7). A mixture of [OsBr(PPh_3)$_2$(η-C_5H_5)] (100 mg, 0.12 mmol) and dfppp (220 mg, 0.13 mmol) was heated in xylenes at 120 °C for 5 days. The xylenes were then removed in vacuo, leaving a yellow residue. This was dissolved in CH_2Cl_2/Et_2O and left at −30 °C for 12 h. A brown decomposition product was removed by filtration, and the filtrate was subjected to preparative TLC on silica (15% acetone/85% hexane). The major yellow band was collected and extracted with CH_2Cl_2, and the solution thus obtained was evaporated to dryness, leaving compound **7** as a yellow powder (52 mg, 0.026 mmol, 21%). ^{1}H NMR ($CDCl_3$): δ 7.7−7.2 (m, 16H, Ar−H), δ 4.7 (s, 5H, C_5H_5), δ 3.2 (m, 2H, PCH_2), δ 2.8 (m, 2H, P′CH_2), δ 2.6 (m, 1H, PCH_2CHCH_2P′), δ 1.7 (m, 1H, PCH_2CHCH_2P′). ^{31}P{^{1}H} NMR ($CDCl_3$): −8.6 (s). ^{13}C{^{1}H} NMR ($CDCl_3$): δ 143.0 (m, C_{ispo}), δ 133.0 (at, C_{ortho}), δ 132.4 (at, C'_{ortho}), δ 130.4 (t, $^2J_{C-F}$ = 25 Hz, C_{para}), δ 129.9 (t, $^2J_{C-F}$ = 25 Hz, C'_{para}), δ 126.4 (m, C_{meta}), δ 120−108 (m, C_6F_{13} tails), δ 77.1 (s, Cp), δ 23.1 (at, J_{C-P} = 18 Hz, PCH_2), δ 22.0 (s, CH_2). MS (FAB$^+$): 2020 [M]$^+$, 1941 [M − Br]$^+$.

Synthesis of [OsBr(dfppe)(η-C_5H_5)] (8). A mixture of [OsBr(PPh_3)$_2$(η-C_5H_5)] (210 mg, 0.24 mmol) and dfppe (400 mg, 0.24 mmol) was heated in xylenes (40 mL) at reflux for 5 h. After cooling to room temperature, this solution was reduced to 10 mL, depositing an orange oil. The mother liquor was decanted, and to this oil was added CH_2Cl_2 and *n*-hexane. This yellow solution was reduced on a rotary evaporator until a precipitate formed, when the flask was cooled to −30 °C for 12 h. The resulting yellow precipitate was then filtered and washed with cold cyclohexane, affording complex **8**, dried in vacuo (103 mg, 0.049 mmol, 20%). ^{1}H NMR ($CDCl_3$): δ 8.0−7.1 (m, 16H, Ar−H), δ 4.7 (s, 5H, C_5H_5), δ 2.7 (m, 4H, PCH_2CH_2P), δ 1.3 (m, 8H, CH_2 of *n*-hexane), δ 0.9 (m, 6H, CH_3 of *n*-hexane). ^{31}P{^{1}H} NMR ($CDCl_3$): 46.1 (s). ^{13}C{^{1}H} NMR ($CDCl_3$): δ 145.7 (d, J = 50 Hz, C_{ipso}), δ 136.8 (d, J = 50 Hz, C'_{ipso}), δ 134.2 (vt, C_{ortho}), δ 130.9 (vt, C'_{ortho}), δ 130.1 (m, C_{para}), δ 126.6 (m, C_{meta}), δ 120−108 (m, C_6F_{13} tails), δ 77.1 (s, C_5H_5), δ 23.0 (vt, J_{C-P} = 18 Hz, PCH_2), δ 21.8 (s, CH_2). MS (FAB$^+$): 2005 [M]$^+$, 1927 [M − Br]$^+$. Anal. Calcd. for $C_{55}H_{25}BrF_{52}P_2Os\cdot(CH_3(CH_2)_4CH_3)$: C, 35.02; H, 1.88. Found: C, 34.65; H, 1.72.

Structure Determinations. Full spheres of CCD area-detector diffractometer data were measured (ω-scans, monochromatic Mo Kα radiation, λ = 0.7107$_3$ Å), yielding $N_{t(otal)}$ reflections, these merging to N unique (R_{int} cited) after "empirical"/multiscan absorption correction (proprietary software), N_o with $I > 2\sigma(I)$ being considered "observed". The large block least-squares refinements on F^2 (all data), refined anisotropic displacement parameter forms for the non-hydrogen atoms, (x, y, z, U_{iso})$_H$ being included following a riding model. Conventional residuals at convergence are cited (weights: $(\sigma^2(F)^2 + (aP)^2 (+ bP))^{-1}$; $P = (F_o^2 + 2F_c^2)/3$); Neutral atom complex scattering factors were employed within the SHELXL 97 program system.[34] Crystal and refinement data are collected in Table 1. Results are presented below and in the figures and tables, selected geometries in Table 2. In the figures, non-hydrogen atoms are shown with 50% probability amplitude displacement envelopes, hydrogen atoms (where shown) having arbitrary radii of 0.1 Å. Full details (excluding structure factor amplitudes) are recorded as Cif depositions with the Cambridge Crystallographic Data Base, CCDC 693355−693357.

It is convenient to gather together here for comparative purposes[35] data on *trans*-[$RuCl_2$(dppx)$_2$] systems ("dppx" = $Ph_2P(CH_2)_xPPh_2$; x = 1 ("dppm"), 2 ("dppe"), 3 ("dppp"), which have been the subject of previous[36−41] and current studies.)

Results and Discussion

Syntheses. The weakly coordinated DMSO ligands were readily displaced from [$RuCl_2$(DMSO)$_4$] by the bidentate ligand dfppp, ($F_{13}C_6C_6H_4$-*p*)$_2$P(CH_2)$_3$P(*p*-$C_6H_4C_6F_{13}$)$_2$, 1,3-bis[(difluoroponytail)phosphino]propane, to give exclusively *trans*-[$RuCl_2$(dfppp)$_2$] (**1**) in 80% yield. The analogous reaction with dfppe, ($F_{13}C_6C_6H_4$-*p*)$_2$P(CH_2)$_2$P(*p*-$C_6H_4C_6F_{13}$)$_2$, 1,2-bis[(difluoroponytail)phosphino]-ethane, gave [$RuCl_2$(dfppe)$_2$] (**2**) which, by comparison, was a mixture of geometric isomers in a 3:1 cis/trans ratio (cf. the nonfluorous analog [$RuCl_2$(dppe)$_2$], where it was also isolated in a 3:1 cis/trans ratio[13]); the pure cis complex

(34) Hall, S. R.; de Boulay, D. J; Olthof-Hazekamp R. *The Xtal 3.7 System*; University of Western Australia: Perth, 2001.

(35) In the course of the present and related work, the parent dppe and dppp materials have been crystallized in new solvate forms and are recorded herein (CCDC 693358−693360); ***trans*-[$RuCl_2$(dppe)$_2$]·$2CH_2Cl_2$** ≡ $C_{54}H_{52}Cl_6P_4Ru$; M = 1138.7; monoclinic, space group $P2_1/c$ (C_{2h}^5, No. 14); a = 11.211(3), b = 13.250(3), c = 16.872(4) Å; β = 97.069(5)°; V = 2487 Å^3; T ∼ 153 K; D_{calcd} (Z = 2) = 1.52$_0$ g cm^{-3}; μ_{Mo} = 0.80 mm^{-1}; specimen, 0.10 × 0.09 × 0.04 mm; "T"$_{min/max}$ = 0.77; $2\theta_{max}$ = 60°; N_t = 29344, N = 6489 (R_{int} = 0.14), N_o = 2802; R1 = 0.069, wR2 = 0.016 (a = 0.068). The solvent was modelled as disordered over two sets of sites, occupancies refining to 0.752(5) and complement. The structure is "isomorphous" with its Ru/thf,[40] V/thf,[68] Rh/EtOH,[69] Re/thf,[70] and Re/Me_2CO[71] counterparts, the present being refined in the same cell and coordinate setting as the latter. The result was considered curious in the light of the record of a similar solvate,[39] $C2/c$, and the possibility explored that the pair of results were of the same system, monoclinic, b being 13.250(3) Å and V being 2487 Å^3 (ca. 153 K) for the present $P2_1/c$ model, 13.85(1) Å and 4959 Å^3 (ca. 295 K) for the $C2/c$. The conjecture was rejected upon (e.g.) consideration of the two cell projections down b, wherein it is evident (e.g.) that the Cl−Ru−Cl lines (centrosymmetric in both structures) differ markedly in their inclinations to b. The possibility of modification of one or other of the crystallization solvent components may account for the different forms, the present material being crystallized from dichloromethane/ethanol. ***trans*-[$RuCl_2$(dppe)$_2$]·$4CHCl_3$** ≡ $C_{56}H_{52}Cl_{14}P_4Ru$, M = 1446.3; triclinic, space group $P\bar{1}$ (C_i^1, No. 2); a = 12.390(2), b = 14.139(2), c = 20.016(3) Å; α = 100.804(3); β = 102.493(4), γ = 111.468(4)°; V = 3046 Å^3; T ∼153 K; D_{calcd} (Z = 2) = 1.57$_7$ g cm^{-3}; μ_{Mo} = 1.01 mm^{-1}; specimen, 0.37 × 0.26 × 0.15 mm; "T"$_{min/max}$ = 0.66; $2\theta_{max}$ = 75°; N_t = 59554, N = 30232 (R_{int} = 0.030), N_o = 22912; R1 = 0.036, wR2 = 0.097(a = 0.046). (x, y, z, U_{iso})$_H$ refined throughout. A previous deposition of this structure has been made; the present rather precise determination defines interesting hydrogen bonding between the substrate chloride and chloroform hydrogen atoms. ***trans*-[$RuCl_2$(dppp)$_2$]·$5CH_2Cl_2$** ≡ $C_{59}H_{62}Cl_{12}P_4Ru$, M = 1421.6; monoclinic, space group $C2/c$ (C_{2h}^6, No. 15); a = 12.593(1), b = 26.342(3), c = 18.963(2) Å; β = 96.033(2)°; V = 6256 Å^3; D_{calcd} (Z = 4) = 1.50$_9$ g cm^{-3}; μ_{Mo} = 0.90 mm^{-1}; specimen, 0.40 × 0.30 × 0.25 mm; "T"$_{min/max}$ = 0.60; $2\theta_{max}$ = 50°; N_t = 63814, N = 5339 (R_{int} = 0.068), N_o = 4695; R1 = 0.072, wR2 = 0.17 (a = 0.048, b = 0.102). Displacement parameters on the solvent molecules were high, but no disorder was resolvable. Hydrogen bonding is found between substrate Cl(1) and H_2CCl_2(3) and between Cl(2) and H_2CCl_2(1).

(36) Chakravarty, A. R.; Cotton, F. A.; Schwotzer, W. *Inorg. Chim. Acta* **1984**, *84*, 179.

(37) Fontes, M. R. M.; Oliva, G.; Cordeiro, L. A. C.; Batiste, A. A. *J. Coord. Chem.* **1993**, *30*, 125.

(38) Fronczek, F. R.; Breaux, H.; McBride, T. G.; Srivastava, R. S. Cambridge Crystallographic Data Base, private communication ("RALLUL").

(39) Lobana, T. S.; Singh, R.; Tiekink, E. R. T. *J. Coord. Chem.* **1990**, *21*, 225.

(40) Chang, C.-W.; Ting, P.-C.; Lin, Y.-C.; Lee, G.-H.; Wang, Y. *J. Organomet. Chem.* **1998**, *553*, 417.

(41) Polam, J. R.; Porter, L. C. *J. Coord. Chem.* **1993**, *29*, 109.

Table 1. Crystal/Refinement Data, [RuCl(dfppp)(η-C_5H_5)] (**5**), and *trans*-[$RuCl_2$-(^{F}P^P^F)$_2$] (·*n*S)

^{F}P^P^F (compound)	dfppp(**5**)[a]	dfppp (**1**)[b]	dfppe (**2**)[c]
*n*S	$CHCl_3 \cdot 1/2C_5H_{12}$	$0.5CHCl_3$	
formula	$C_{59.5}H_{34}Cl_4F_{52}P_2Ru$	$C_{102.5}H_{44.5}Cl_{3.5}F_{104}P_4Ru$	$C_{100}H_{40}Cl_2F_{104}P_4Ru$
M_r (Da)	2041.7	3600.9	3513.2
cryst syst	triclinic	triclinic	triclinic
space group	$P\bar{1}$ (#2)	$P\bar{1}$ (#2)	$P\bar{1}$ (#2)
a (Å)	11.933(2)	16.595(2)	12.986(2)
b (Å)	22.773(3)	20.796(3)	15.406(2)
c (Å)	28.434(4)	21.699(3)	16.703(3)
α (Å)	82.934(3)	107.103(2)	76.908(2)
β (Å)	87.744(3)	105.130(2)	68.784(2)
γ (Å)	76.751(3)	109.180(2)	80.123(2)
V (Å^3)	7464	6207	3019
D_{calcd} (g cm^{-3})	1.81_7	1.92_7	1.93_2
Z	4	2	1
μ_{Mo} (mm^{-1})	0.57	0.46	0.44
specimen (mm^3)	0.50, 0.15, 0.10	0.28, 0.24, 0.16	0.43, 0.37, 0.13
'*T*'$_{min/max}$	0.086	0.87	0.92
$2\theta_{max}$ (deg)	58	50	56
N_t	68795 (0.044)	45445	25850
N (R_{int})	32642	21719 (0.040)	13620 (0.024)
N_o	17790	13086	10265
R1	0.11	0.069	0.074
wR2 (a,b)	0.28(0.080, 65)	0.24 (0.109, 21))	0.23 (0.123, 8.75)
T (K)	170	153	170

[a] The outer components of "tails" 12n, 22n, and 42n were modeled as disordered over two sets of sites, seemingly concerted, occupancies refining to 0.627(6) and complement. [b] The solvent molecule was modeled as disordered about a crystallographic inversion center; tail 24n was modeled as disordered over two sets of sites, occupancies set at 0.5 each after trial refinement. [c] Peripheral components of tail 34n were modeled as disordered over two sets of sites, occupancies set at 0.5 after trial refinement.

was obtained by recrystallization from Et_2O/hexane. An alternative route to complex **2** involved the reaction of [$RuCl_2(PPh_3)_3$] with 2 equiv of dfppe in ethanol at room temperature, also giving a mixture of *cis*/*trans*-[$RuCl_2$-(dfppe)$_2$]. The corresponding *trans*-[OsX_2(dfppp)$_2$] compounds were prepared by the displacement of triphenylphosphine from [$OsX_2(PPh_3)_3$] where X = Br (**3**) and Cl (**4**). The *trans*-osmium isomer preferentially precipitates from solution for both halide derivatives, as was confirmed by ^{31}P NMR spectroscopy. A separate reaction between [$OsBr_2(PPh_3)_3$] and 2 equiv of dfppp was conducted over five days. The presence of both *cis*- and *trans*-[$OsBr_2$(dfppp)$_2$] was detected after separation by preparative TLC, then spectroscopic confirmation of the separated bands. In all cases, the particular isomer of [MX_2P_4], M = Ru, Os; X = halide, that forms is highly dependent on the reaction conditions and the diphosphine employed. For example, the isolation of exclusively *cis*-[$RuCl_2$(depe)$_2$] in 95% yield has been reported (depe = 1,2-bis(diethylphosphino)ethane).[14] The kinetic product, which is generally the *trans*-isomer, can be thermally converted to the cis isomer, which is the thermodynamic product. Isomerization can also be achieved by electrochemical or photochemical methods.[42]

The *trans*-[MX_2(dfppp)$_2$] complexes exhibited excellent solubility in Et_2O yet were only slightly soluble in chloroform and acetone and were insoluble in tetrahydrofuran (thf). In stark contrast, the nonfluorous analog [$RuCl_2$(dppp)$_2$] was readily dissolved in thf, acetone, and chloroform and was insoluble in Et_2O.

Since the original report of a high-yielding synthesis of [$RuCl(PPh_3)_2(\eta$-$C_5H_5)$],[43] a wide variety of complexes have been made from this precursor by displacement of the labile triphenylphosphine (PPh_3) ligands. Complexes of the type [RuCl(diphosphine)(η-C_5H_5)] have been applied as efficient catalysts for numerous reactions,[10,44] including hydrogen transfer from alcohols to ketones.[45] The reaction of [$MX(PPh_3)_2(\eta$-$C_5H_5)$] with fluorous diphosphines ^{F}P^P^F gave [$MX(^F$P^P$^F)(\eta$-$C_5H_5)$] for M = Ru; X = Cl; ^{F}P^P^F = dfppp (**5**) and dfppe (**6**) and M = Os; X = Br; ^{F}P^P^F = dfppp (**7**) and dfppe (**8**). The ruthenium complexes were synthesized in refluxing toluene, while formation of the osmium complexes was generally slower and required refluxing xylenes. All complexes displayed similar properties and were isolated as yellow, relatively air-stable solids, but solutions regularly decomposed to brown/black oils on exposure to the air. The complexes showed good solubility in all organic solvents and were only insoluble in water. In an effort to ensure that the samples were not contaminated with PPh_3, chromatographic separation was generally employed. However, it was later discovered that the complexes could be preferentially precipitated from a mixture of CH_2Cl_2 and *n*-hexane, leaving PPh_3 in solution.

The excellent solubilities of the cyclopentadienyl complexes in organic solvents were in stark contrast to those of the [MX_2(dfppp)$_2$] complexes, which only exhibited good solubilities in diethyl ether. This is not surprising, however, upon visualization of the three-dimensional structures of [MX_2(dfppp)$_2$] compared to [MX(dfppp)-(η-C_5H_5)]. The former, with eight fluoro-ponytails, possess a fluorous "shell", which presumably governs the overall molecular solubility. The fluoro-ponytails in the cyclopentadienyl complexes are spread extensively in space, resulting in the presence of large, nonfluorous areas for solvents to penetrate, as is exemplified by the presence of *n*-pentane and chloroform in the crystal structure of [RuCl(dfppp)(η-C_5H_5)] (vide infra). In general, the solubility behavior of the new highly fluorous complexes was often hard to predict. Comparisons to nonfluorous analogs such as [$RuCl_2$(dppe)$_2$] were also difficult given that this compound will readily dissolve in CH_2Cl_2, acetone, or thf, while the fluorous counterpart [$RuCl_2$(dfppe)$_2$] would not dissolve in any of these solvents and was only appreciably soluble in Et_2O.

Spectroscopic Properties Of The Complexes. Incorporation of the aromatic units between the phosphorus atoms and the C_6F_{13} tails was hoped to reduce the electron-withdrawing effect of the perfluoroalkyl groups. Synthetically, the ligands have shown to behave in a similar fashion to the nonfluorous diphosphine analogs, forming metal chelate complexes readily. Closer examination by ^{31}P NMR shows that the chemical shifts of the fluorous complexes *trans*-[$RuCl_2$(dfppx)$_2$] (**1** and **2**) are

(42) Sullivan, B. P.; Meyer, T. J. *Inorg. Chem.* **1982**, *21*, 1037.
(43) Ashby, G. S.; Bruce, M. I.; Tomkins, I. B.; Wallis, R. C. *Aust. J. Chem.* **1979**, *32*, 1003.
(44) van der Drift, R. C.; Vailati, M.; Bouwman, E.; Drent, E. *J. Mol. Catal. A: Chem.* **2000**, *159*, 163.
(45) Pamies, O.; Backvall, J.-E. *Chem.—Eur. J.* **2001**, *7*, 5052.

Table 2. Selected Geometries for Complexes **1** and **2** (and Other $[RuCl_2(dppx)_2]$ Comparators)

dppx (cpd.)	dfppp(**1**) (mol 1)	dfppp(**1**) (mol 2)	dfppe(**2**)	dppm[a]	dppe[b]	dppe[c]	dppp[d]
			Distances (Å)				
Ru−Cl	2.444(1)	2.442(1)	2.435(1)	2.426(1)	2.430(1)	2.4150(5), 2.4367(5)	2.398(2), 2.427(2)
Ru−P	2.385(1), 2.453(1)	2.401(1), 2.452(1)	2.360(1), 2.384(1)	2.340(1), 2.367(1)	2.354(2) 2.383(2)	2.3713(4) 2.3933(5)	2.411(1), 2.412(2)
average	2.42(3)		2.37(2)	2.35(2)	2.37(2)	2.387(11)	2.411(2)
			Angles (deg)				
Cl−Ru−P	79.27(4) −100.73(4)	80.32(4) −99.68(4)	82.48(4) 97.52(4)	80.77(4) −99.23(4)	80.13(6) −99.87(6)	85.77(2) −94.15(2)	83.50(4) −96.50(4)
Cl−Ru−X	180(−)	180(−)	180(−)	180(−)	180(−)	176.18(1)	180(−)
P−Ru−P(bite)	85.71(4)	85.86(4)	81.27(4)	71.39(4)	81.53(5)	83.05(2), 83.29(2)	86.32(5)
P−Ru−P(trans)	180(−)	180(−)	180(−)			174.79(1), 175.26(2)	167.04(7), 168.93(7)
P−Ru−P(cis)	94.29(4)	94.14(4)	98.73(4)	108.61(4)	98.47(5)	95.97(2), 98.11(2)	94.93(5)

[a] Ref 36. [b] (Present) CH_2Cl_2 solvate; [c] (Present) $CHCl_3$ solvate; as noted in the footnote,[35,38] there are strong hydrogen bonds from the chloroform solvate hydrogens to both chlorines. [d] (Present) CH_2Cl_2 solvate; as noted in the footnote, hydrogen bonds are found from each of the coordinated chlorine atoms to solvate molecules.

only slightly downfield of the nonfluorous complexes *trans*-$[RuCl_2(dppx)_2]$ (Table 3). Thus, the aryl spacers have insulated the phosphorus atoms from most of the electron-withdrawing effect of the C_6F_{13} groups, but not completely. Hope and co-workers have previously observed a similar phenomenon.[46] In spite of the bulk of the fluorinated tails, very little distortion of the RuP_4 core seems to have occurred (Table 2), and thus there must be little contribution to the chemical shift from these potential distortions.

Table 3 shows the shielding effect as one descends the group, which is a well-known phenomenon[47] and for example has been observed by Tolman in the series of complexes [(2-naphthyl)HM(dmpe)$_2$] (M = Fe, Ru, Os).[48] Complexes **1**−**4** in their trans geometry all exhibited singlet resonances in their $^{31}P\{^1H\}$ NMR spectra assigned to the equivalent fluorodiphosphines. Complex *cis*-**2** had the expected two signals at 49 and 62 ppm.

The most significant features of the ^1H NMR spectra of **1**−**4** are the aromatic protons at ca. 7.4 ppm and the hydrocarbon bridge between the phosphorus atoms at ca. 2−3 ppm, accompanied by coupling to the phosphorus atoms.

The aromatic region of the $^{13}C\{^1H\}$ NMR spectrum of **1** contained signals at δ 134.8, 130.9, 130.5, and 125.7 ppm. A DEPT experiment assigned the signals at 130.9 and 130.5 as quaternary carbon atoms. The former, assigned to C_{ipso}, exhibited a one-bond coupling to phosphorus, with $^1J_{C-P}$ = 10 Hz. The latter, assigned to C_{para}, was a triplet, and its multiplicity arose from two-bond coupling to fluorine, with $^2J_{C-F}$ = 25 Hz. A series of multiplets resonating between 121 and 108 ppm was assigned to the C_6F_{13} tails. The other signals at δ 27.5 and 19.2 ppm were assigned as the PCH_2 and central CH_2 groups of the $PCH_2CH_2CH_2P$ bridge, respectively. This spectrum was representative of the other two complexes **2** and **4**, complex **3** being too insoluble to obtain an adequate spectrum.

Table 3. NMR Data for Fluorous Complexes (Shifts in Regular Font) and Some Non-Fluorous Analogs (Shifts in *Italics*)[a]

compound	$\delta(^{31}P)$	$\delta(^1H)$ C_5H_5	$\delta(^{13}C)$ C_5H_5
trans-$[RuCl_2(dfppp)_2]$(**1**)[b]	−2.1		
trans-$[RuCl_2(dppp)_2]$[c]	*−4.8*		
trans-$[RuCl_2(dfppe)_2]$(**2**)[d]	52		
cis-$[RuCl_2(dfppe)_2]$(**2**)	62, 49		
trans-$[RuCl_2(dppe)_2]$[c]	*45.6*		
trans-$[OsBr_2(dfppp)_2]$(**3**)[e]	−55.0		
trans-$[OsCl_2(dfppp)_2]$(**4**)[d]	−47.5		
$[RuCl(dfppp)(\eta\text{-}C_5H_5)]$(**5**)[b]	40.8	4.5	81.2
$[RuCl(dfppe)(\eta\text{-}C_5H_5)]$(**6**)[f]	82.1	4.6	81.0
$[RuCl(dppe)(\eta\text{-}C_5H_5)]$[g]	*79.7*	*4.6*	
$[OsBr(dfppp)(\eta\text{-}C_5H_5)]$(**7**)[b]	−8.6	4.7	77.1
$[OsBr(dfppe)(\eta\text{-}C_5H_5)]$(**8**)[b]	46.1	4.7	77.1

[a] All ^{31}P chemical shifts referenced to external H_3PO_4. ^1H chemical shifts were referenced to incompletely deuterated solvent signals; ^{13}C chemical shifts were referenced to the deuterated solvents. [b] Experiments performed in $CDCl_3$. [c] Performed in $CDCl_3$, ref 50. [d] Experiments performed in d_6-acetone. [e] Performed in diethyl ether, unlocked. [f] Performed in CD_2Cl_2. [g] Performed in $CDCl_3$, ref 43.

The complexes $[MX(^FP\text{^}P^F)(\eta\text{-}C_5H_5)]$, **5**, **6**, **7**, and **8**, have NMR spectra that show sharp resonances for the cyclopentadienyl ligand at ca. 4.6 ppm in their ^1H NMR spectra and at ca. 81 ppm (for Ru) and 77 ppm (for Os) in their $^{13}C\{^1H\}$ NMR spectra.

The ^1H and ^{13}C NMR spectra of **5** indicate an asymmetry in the backbone of the chelate Ru(dfppp), as found in its crystal structure. The six atoms contained in this chelate ring have a typical "chair" conformation normally associated with cyclohexane rings, and as such, the $PCH_2CH_2CH_2P$ bridge contains chemically inequivalent axial and equatorial hydrogen atoms. This phenomenon was observed in complexes **5**−**8** and in the complex $[MnCl(CO)_3(Ph_2PCH_2CMe_2CH_2PPh_2)]$,[49] where

(46) Bhattacharyya, P.; Gudmunsen, D.; Hope, E. G.; Kemmit, R. D. W.; Paige, D. R.; Stuart, A. M. *J. Chem. Soc., Perkin Trans. 1* **1997**, 3609.
(47) Garrou, P. E. *Chem. Rev.* **1981**, *81*, 229.
(48) Tolman, C. A.; Ittel, S. D.; English, A. D.; Jesson, J. P. *J. Am. Chem. Soc.* **1978**, *100*, 4080.
(49) Kraihanzel, C. S.; Ressner, J. M.; Gray, G. M. *Inorg. Chem.* **1982**, *21*, 879.

the CMe_2 backbone methyl resonances exhibited different chemical shifts.

Analysis of **1**−**8** by either high-resolution ESI or FAB mass spectrometry gave ions assigned to $[M]^+$ and $[M - \text{halide}]^+$, in general, with little fragmentation.

Electrochemistry Studies. Another way to probe the electronic properties of these highly fluorous complexes is with cyclic voltammetry. The electron-withdrawing ability of the C_6F_{13} tails may manifest itself through the oxidation potential of the group 8 M^{II}/M^{III} couple. The half-sandwich compounds each show a one-electron, quasi-reversible oxidation versus the ferrocene couple (Table 4). This is in general agreement with the one-electron oxidations that $[RuHL_2(\eta\text{-}C_5H_5)]$ (L = PPh_3; L_2 = dppm, dppe, and dppp) undergo[50] (Table 4), albeit with slightly different electrochemical conditions (different solvent system, but $E_{1/2}$ values still relative to ferrocene). It is plausible that the impact of only one fluorous phosphine ligand in these complexes does not manifest itself with an increased oxidation potential of the metal atom. On the other hand, the oxidation potentials of the *trans*-$[MCl_2(dfppp)_2]$ (M = Ru, Os) complexes are higher than the nonfluorous derivatives (Table 4). This may indicate that the eight C_6F_{13} tails do exert some electron-withdrawing influence on the metal atom. In addition, the longer diphosphine backbone in the fluorous complexes compared with the nonfluorous analogs may also contribute to the differences in oxidation potentials.

Single-Crystal X-Ray Structure Determinations of $[RuCl_2(dfppp)_2]$ (1), $[RuCl_2(dfppe)_2]$ (2), and $[RuCl(dfppp)(\eta\text{-}C_5H_5)]$ (5). The results of the single-crystal X-ray structure determinations of **1** (Figure 2), **2**, and **5** (Figure 3) are consistent in terms of stoichiometry and connectivity with the proposed formulations. Additionally, complexes **1** and **5** have various molecules of solvation present in the lattice. Complexes **1** and **2** are disposed with their ruthenium atoms on crystallographic centers of symmetry. In **2**, one-half molecule and, in **1**, two independent half-molecules comprise the asymmetric units of their respective structures, which, in the case of **1**, also includes a chloroform molecule of solvation, disordered about an inversion center. Core geometries for the new complexes reported in this work and related nonfluorous dppx derivatives are presented in Table 2. The trends for the nonfluorous complexes are reflected in the fluorinated analogs with the significant difference that, in the $P(CH_2)_3P$ complexes, the conformations of the chelate rings in **1** are close to *m* (passing through Ru and the central carbon atom), while in $[RuCl_2(dppp)_2]$, a quasi-2 axis passes through those atoms. Notwithstanding the quasi-*m* symmetry of the chelate ring in **1**, there are great disparities in the associated P−Ru−Cl angles, echoed in a number of other derivatives, possibly reflecting the differing associated phenyl ring dispositions and their proximity to the chlorine atom. The conformations of all of the $P(CH_2)_2P$ systems cited are quasi-2. For **5**, two formula units, devoid of crystallographic symmetry, and solvated with chloroform and pentane molecules, comprise the asymmetric unit of the structure; core geometries, counterparts, are presented in Figure 3. There being no closely similar comparator available for the $(CH_2)_3$ system, it is of interest to consider the present in the context of the $(CH_2)_{1,2}$ systems, Ru−Cl, P, and C(0) (= C_5H_5 centroid) being closely similar (as are the Ru−C(C_5H_5) ranges), while, among the angles, the dppx "bite" angle is the only descriptor varying by any substantial amount, the consequences of that change being absorbed fairly evenly among the remaining angles. The chelate ring again takes the *m* conformation.

A search of the Cambridge Crystallographic Database[53] revealed only a small number of complexes containing relatively long perfluorinated chains attached to the metal complex ligand scaffolds. In particular, it appears that, to the best of our knowledge, only one other structure has been determined which includes a diphosphine ligand containing fluoroponytails[54] which coordinates in a tridentate fashion through CH activation of the hydrocarbon linker. Given that many waxes and lubricants used in industry require perfluorocarbons,[55] it was not surprising that we experienced many difficulties in effectively crystallizing such materials, as they often preferred to deposit as oils. The two molecules of complex **1** differ very little in overall geometry, but when the symmetry-equivalent portions of the molecules are considered, they appear to pack to form an embracing dimer, presumably as a result of packing in the lattice. The structure was analyzed using Hirshfeld surfaces, implemented in *Crystal Explorer 2.1*, where the authors of this program have provided a means of analyzing intermolecular interactions using "a whole-of-molecule

Table 4. Cyclic Voltammetry of the Complexes (Non-Fluorous Compounds in Italics)

	complex	$E_{1/2}$ (V)	E^{ox} irrev. (V)
1	*trans*-$[RuCl_2(dfppp)_2]$		0.88
4	*trans*-$[OsCl_2(dfppp)_2]$		0.99
	trans-$[RuCl_2(dppm)_2]$	*0.42*[a]	
		0.52[b]	
	trans-$[RuCl_2(dppe)_2]$	*0.60*[c]	
		0.56[d]	
	trans-$[OsCl_2(dppm)_2]$	*0.18*[e]	
	trans-$[OsCl_2(dppe)_2]$	*0.22*[f]	
5	$[RuCl(dfppp)(\eta\text{-}C_5H_5)]$	−0.32	
6	$[RuCl(dfppe)(\eta\text{-}C_5H_5)]$	−0.25	
7	$[OsBr(dfppp)(\eta\text{-}C_5H_5)]$	−0.20	
8	$[OsBr(dfppe)(\eta\text{-}C_5H_5)]$	−0.10	
	$[RuH(PPh_3)_2(\eta\text{-}C_5H_5)]$	*−0.28*	
	$[RuH(dppm)(\eta\text{-}C_5H_5)]$		*-0.08*
	$[RuH(dppe)(\eta\text{-}C_5H_5)]$	*−0.16*	
	$[RuH(dppp)(\eta\text{-}C_5H_5)]$	*−0.26*	

[a] Measured in acetonitrile/0.1 M Bu_4NPF_6, versus saturated NaCl calomel electrode.[18] [b] Measured in dichloromethane/0.2 M Bu_4NBF_4, versus Ag/AgCl electrode.[51] [c] Measured in dichloromethane/0.1 M Bu_4NPF_6, versus F_c/F_c^+ at 0.56 V.[52] [d] Measured in dichloromethane/0.2 M Bu_4NBF_4, versus Ag/AgCl electrode.[51] [e] Measured in acetonitrile/0.1 M Bu_4NPF_6, versus saturated NaCl calomel electrode.[18] [f] Measured in dichloromethane/0.1 M Bu_4NPF_6, versus Ag/AgCl electrode.[20]

(50) Smith, K.-T.; Romming, C.; Tilset, M. *J. Am. Chem. Soc.* **1993**, *115*, 8681.

(51) Szczepura, L. F.; Giambra, J.; See, R. F.; Lawson, H.; Janik, T. S.; Jircitano, J.; Churchill, M. R.; Takeuchi, K. J. *Inorg. Chim. Acta* **1995**, *239*, 77.

(52) Powell, C. E.; Cifuentes, M. P.; Morrall, J. P.; Stranger, R.; Humphrey, M. G.; Samoc, M.; Luther-Davies, B.; Heath, G. A. *J. Am. Chem. Soc.* **2003**, *125*, 602.

(53) Allen, F. H. *Acta Crystallogr.* **2007**, *B58*, 380.

(54) de Wolf, E.; Spek, A. L.; Kulpers, B. W. M.; Philipse, A. P.; Meeldijk, J. D.; Bomans, P. H. H.; Frederik, P. M.; Deelman, B.-J.; van Koten, G. *Tetrahedron* **2002**, *58*, 3911.

(55) Lanteri, P.; Longeray, R. *Actualite Chim.* **2004**, *272*, 6.

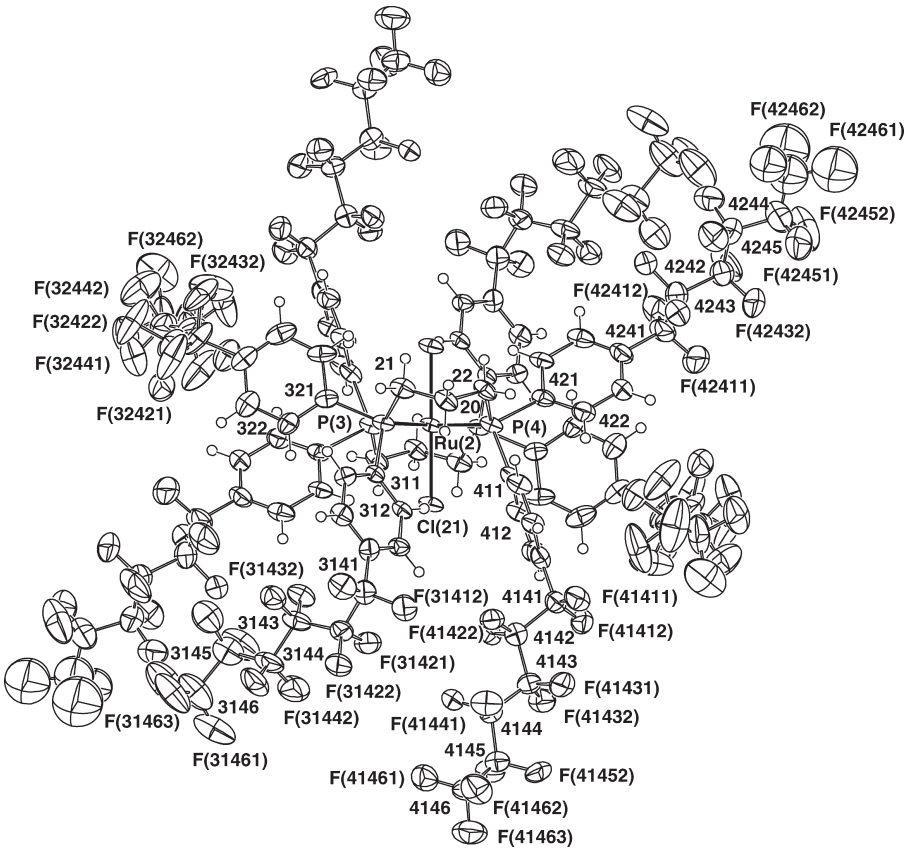

Figure 2. Molecular projection of complex **1**.

approach".[56] The use of a normalized contact distance, d_{norm}, from points on the Hirshfeld surface to the nearest atoms outside and inside the surface takes into account the sizes of the atoms and incorporates comparisons to van der Waals (vdW) radii of the atoms and is thus able to highlight contacts longer and shorter than vdW separations. The shorter contacts appear as red focii which increase in intensity as the internuclear separations decrease. The structure of complex **1** can also be represented as the Hirshfeld surface in Figure 4a, where the structure has been modified to remove the disorder and a surface has been constructed about one of the molecules in the asymmetric unit to highlight intermolecular contacts with the other molecule, which is shown "embracing" the surface. While the Hirshfeld surface is dotted with identifiable interactions, they are not very intense, and perhaps these interactions can be attributed to inevitable close approaches as a result of the packing. The information mapped onto Hirshfeld surfaces can also be represented in a two-dimensional map, which summarizes the intermolecular interactions in the crystal and is known as a "fingerprint plot".[56,57] For points on the surface, distances to the nearest atoms outside, d_e, and inside, d_i, are readily defined, and these properties are used, together with the identity of those atoms, to explore the type and the proximity of intermolecular contacts.

Additionally, we can use the fingerprint plot to highlight separate interactions. Complex **1** is highly fluorinated with eight C_6F_{13} chains in the molecule, and this is unique among the structurally characterized fluorous metal complexes. Examination of the packing of these molecules reveals that the perfluoroalkyl chains have a tendency to associate, and intramolecularly, the C_6F_{13} chains maximize their contact. This is telling in the fingerprint plot where ca. 64% of the interactions with the surface are F···F in nature and can be represented by the colored portion of the plot.

The ruthenium geometries of the two molecules in the structure of **1** are similar, Table 1, and also similar to that of complex **2**. These complexes possess essentially trans octahedral stereochemistry with axially coordinating halide ligands and the chelating diphosphine ligands occupying the equatorial sites. The bis-diphosphine complexes are best compared to the analogous diphosphine complexes without fluoro-ponytails, for which a number of these complexes have been characterized structurally, and their data are also collected in Table 2 for comparison.

The structure of **2** has the chains within the molecule also aggregated, and this then extends to the packing in the unit cell, which sees these chains stack in roughly a parallel fashion along *b* (Figure 4b). The fingerprint plot gives F···F interactions amounting to ca. 56% of the total intermolecular interactions.

The structure of **5** also exhibits this now common feature where the fluoroponytails aggregate both inter- and intramolecularly. These two molecules also embrace

(56) McKinnon, J. J.; Jayatilaka, D.; Spackman, M. A. *Chem. Commun.* **2007**, 3814–3816.
(57) Spackman, M. A.; McKinnon, J. J. *CrystEngComm* **2002**, *4*, 378–392.

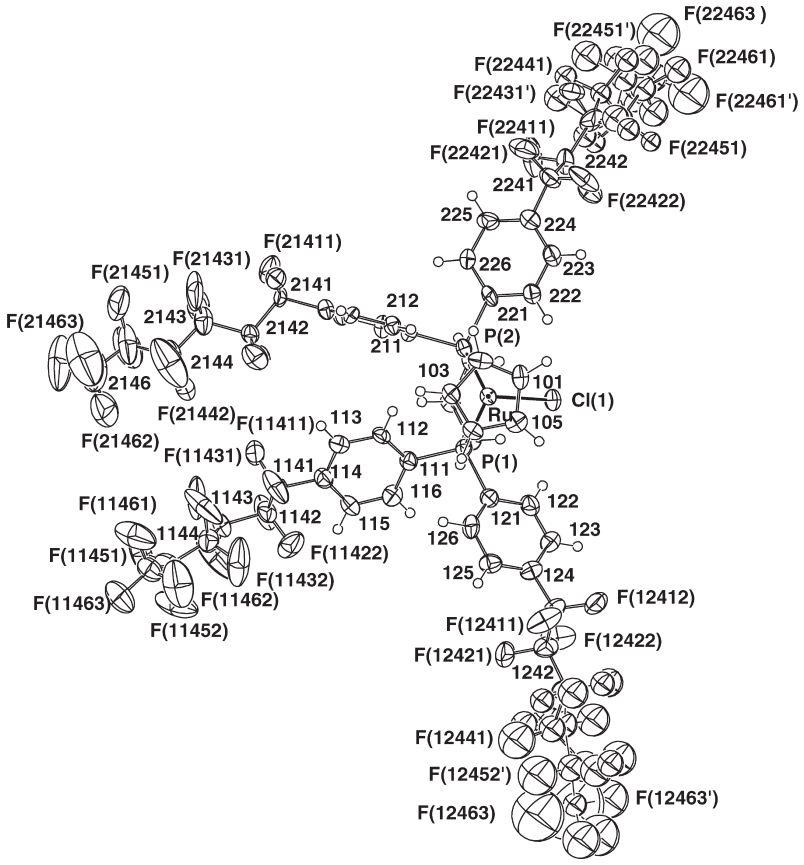

Figure 3. Molecular projection of molecule 1 complex **5**; molecule 2 is similar. Ru−Cl are 2.449(2), 2.443(2) Å; Ru−P 2.279(3), 2.281(2); 2.272(2), 2.280(2) Å; Ru−C(0)(Cp centroid) 1.86_4, 1.85_3 Å.

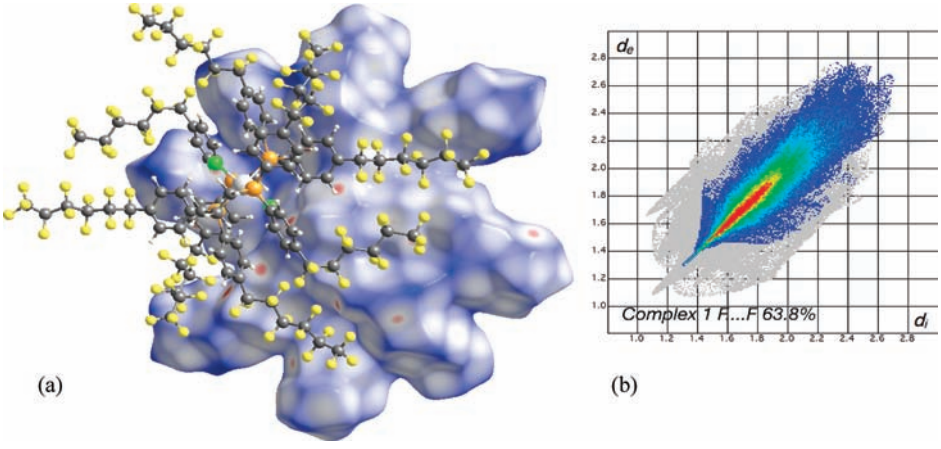

Figure 4. (a) Hirshfeld surface drawn around one molecule in the asymmetric unit of **1**. (b) Fingerprint plot of that surface.

in a similar fashion to **1**, which serves to maximize the dispersive interactions of the fluoroalkyl chains. Furthermore, this structure has additional interactions resulting from the chloroform and pentane solvates. The included pentane occupies a nonfluorous pocket in the unit cell close to a C_6F_{13} chain but beyond the van der Waals distance. The Hirshfeld surface of the pentane solvate shows a significant close contact between the solvate and a cyclopentadienide CH but none with the adjacent fluoroalkyl chain. The fingerprint plot of the pentane molecule gives H···F intermolecular close contacts of ca. 63% and H···H ones of ca. 27%.

The chloroform interactions, on inspection of bond lengths and angles, appear to be significant, exhibiting the range of interactions found for halocarbons. The hydrogen-bonding CH···ClRu interaction is well-known and expected for electronegative elements with accessible lone pairs, that is, halogens acting as hydrogen-bond acceptors.

Potentially more interesting, however, is the possibility of a CCl···C_5H_5(centroid) interaction that can be posited when examining the contact distances. In this case, networks can be constructed such as that depicted in Figure 5 that give the impression of significant contacts.

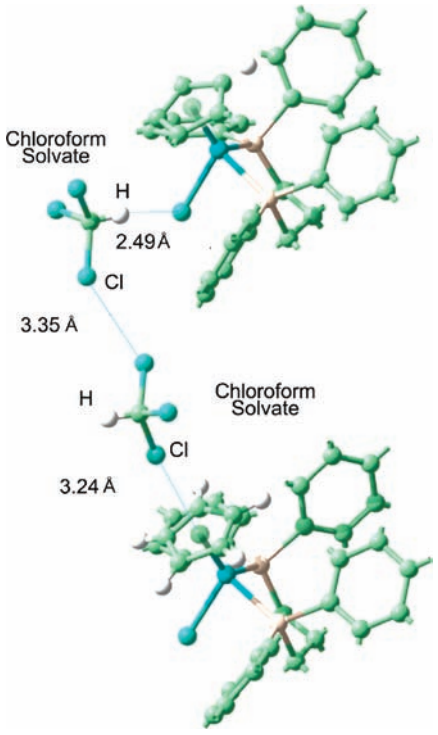

Figure 5. Interaction of the chloroform solvate of complex **5**.

Noncovalent interactions involving halogens have been discussed in the literature extensively.[58−64] The so-called charge-transfer complexes formed between molecular iodine and aromatics such as mesitylene[65,66] were among the first examples that highlighted noncovalent interactions between halogens and aromatic rings. However, halogen-aromatic π-system interactions are not commonly observed, and the possible role of such interactions in more complicated molecular recognition events is not clear.

It is here that the Hirshfeld surface approach shows its worth because the construction of a surface about the chloroform solvate shows definitively that the only significant close contact is the $RuCl\cdots HCCl_3$ hydrogen bond signified by the intense red focus in Figure 6; there are no other intense close contacts. Presumably, the close approach is a consequence of packing in the lattice, and there is no $Cp\cdots HCCl_3$ contact.

Supercritical Carbon Dioxide ($scCO_2$) Solubility Measurements. The solubility measurements in supercritical CO_2 were conducted with a commercial supercritical fluid extractor (SFE). This uses a dynamic method where the supercritical fluid (SCF) passes through the analyte, followed by depressurization and collection of the compound. The solubility can be determined by the mass loss of the analyte from the extraction cell, or the mass of the compound collected. In this work, both masses were measured and were in agreement. Static and chromatographic methods can also be used to determine $scCO_2$ solubility. Static, or equilibrium, methods utilize a solubility cell with transparent windows, and in situ measurement of solubility is performed visually or spectroscopically. Recent work[27] has compared solubility values determined using the SFE with a static solubility measurement (UV−vis spectroscopic detection of the analyte) which showed that the results were comparable. In addition, each solubility measurement in this work was conducted in triplicate, giving a maximum relative standard deviation of 1.3% for the highest solubility values, and 15.4% for the lowest solubility values.

The solubility of *trans*-$[RuCl_2(dfppp)_2]$ (**1**) in $scCO_2$ was determined at a variety of temperatures and pressures (Table 5) and increased with increasing CO_2 density. To a first approximation, the increasing solvent power of a SCF can be related to the increasing solvent density in the critical region.[67] The solubility of $[Co_2(CO)_6\{P(i\text{-}Pr)_2(m\text{-}C_6H_3(CF_3)_2)\}_2]$ (**10**) also increased with increasing CO_2 density (0.7 g/L at a CO_2 density of 0.61 g/mL, to 15.8 g/L at a CO_2 density of 0.82 g/mL).[24]

The solubility measurements of the cyclopentadienyl complexes were performed with a CO_2 density of 0.60 g/mL. At identical conditions, the solubility of **1** was 31 mmol/L and the solubility of **5** was 58 mmol/L. It was expected that **1** would be more soluble than **5** with four more C_6F_{13} tails. This is possibly due to the increased molecular weight of **1** (3541 g/mol) compared with **5** (1886 g/mol), given that in general increasing the molecular weight decreases $scCO_2$ solubility.[67] In addition, the melting point of **1** was 183−185 °C, while **5** melted between 68 and 71 °C. Solubility in $scCO_2$ is dependent upon the vapor pressure of the solute, so **1** would have a much lower vapor pressure than **5**, and this property would certainly contribute to the solubility differences. The highly symmetrical **1** should also contain stronger packing forces compared with **5**, perhaps also contributing to **5** being more soluble than **1** in $scCO_2$. It should be noted that the solubilities in grams per liter of compounds **1** and **5** were equal (1.1 g/L).

$[RuCl(dfppp)(\eta\text{-}C_5H_5)]$ (**5**) displayed a higher solubility compared to $[RuCl(dfppe)(\eta\text{-}C_5H_5)]$ (**6**) (Table 6), possibly due to the increased flexibility of dfppp compared to dfppe, which may slightly weaken the intermolecular forces between molecules of **5** compared to those forces between molecules of **6**. This is confirmed by the melting points of **5** and **6**: **5** melted between 68 and 71 °C, while **6** melted between 78 and 80 °C. Solubility theory

(58) Corradi, E.; Meille, S. V.; Messina, M. T.; Metrangolo, P.; Resnati, G. *Angew. Chem., Int. Ed.* **2000**, *39*, 1782.
(59) Robinson, J. M. A.; Kariuki, B. M.; Harris, K. D. M.; Philp, D. *J. Chem. Soc., Perkin Trans. 2* **1998**, 2459.
(60) Lunghi, A.; Cardillo, P.; Messina, M. T.; Metrangolo, P.; Panzeri, W.; Resnati, G. *J. Fluor. Chem* **1998**, *91*, 191.
(61) Amico, V.; Meille, S. V.; Corradi, E.; Messina, M. T.; Resnati, G. *J. Am. Chem. Soc.* **1998**, *120*, 8261.
(62) Williams, D. E.; Daquan, G. *Inorg. Chem.* **1997**, *36*, 782.
(63) Price, S. L.; Stone, A. J.; Lucas, J.; Rowland, R. S.; Thornley, A. E. *J. Am. Chem. Soc.* **1994**, *116*, 4910.
(64) Bloemink, H. I.; Hinds, K.; Legon, A. C.; Thorn, J. C. *Angew. Chem., Int. Ed. Engl.* **1994**, *33*, 1512.
(65) Lippert, J. L.; Hanna, M. W.; Trotter, P. J. *J. Am. Chem. Soc.* **1969**, *91*, 4035.
(66) Mulliken, R. S. *J. Am. Chem. Soc.* **1950**, *72*, 600.
(67) McHugh, M. A.; Krukonis, V. J. *Supercritical Fluid Extraction - Principles and Practice*; Butterworths: Markham, ON, Canada, 1986.
(68) Holt, D. G. L.; Larkworthy, L. F.; Povey, D. C.; Smith, G. W.; Leigh, G. J. *Inorg. Chim. Acta* **1993**, *207*, 11.
(69) Heaton, B. T.; Jacob, C.; Smith, A. K.; Quayle, M. *Rhodium Express* **1993**, 18.
(70) Al Salih, T.; Duarte, M. T.; Frausto da Silva, J. J. R.; Galvao, A. M.; Guedes da Silva, M. F. C.; Hitchcock, P. B.; Hughes, D. L.; Pickett, C. J.; Pombeiro, A. J. L.; Richards, R. L. *J. Chem. Soc., Dalton Trans.* **1993**, 3015.
(71) Eglin, J. L.; Smith, L. T.; Valente, E. J.; Zubkowski, J. D. *Inorg. Chim. Acta* **1998**, *268*, 151.

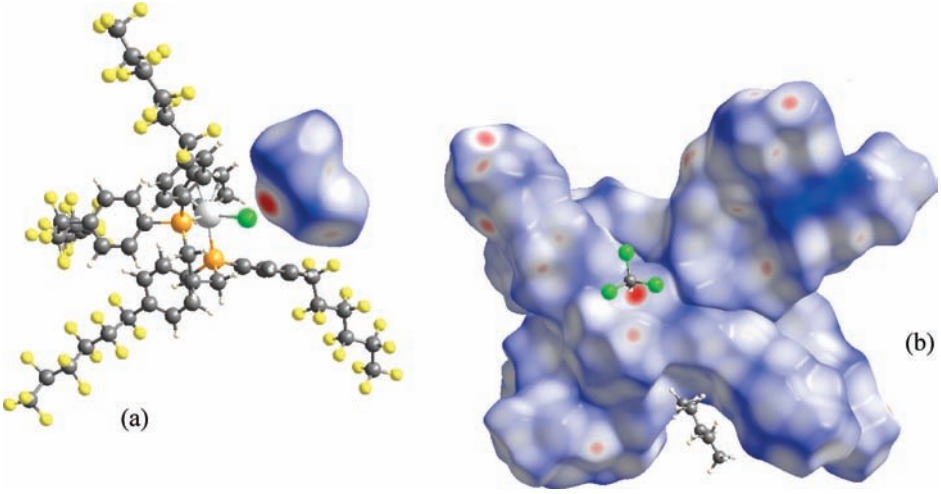

Figure 6. (a) Chloroform solvate Hirshfeld surface with its H-bonding partner. (b) Hirshfeld surface of both molecules in the asymmetric unit and solvent molecules.

Table 5. Supercritical CO_2 Solubility of *trans*-[$RuCl_2$(dfppp)$_2$], **1**

CO_2 density (g/mL)	pressure (bar)	temp. (°C)	concentration (mol/L)	concentration (g/L)
0.50	91	40	0	0
0.50	110	50	1.7×10^{-4}	0.6
0.50	129	60	3.1×10^{-4}	1.1
0.55	93	40	8.5×10^{-5}	0.3
0.60	97	40	3.1×10^{-4}	1.1
0.65	104	40	9.6×10^{-4}	3.4
0.80	164	40	2.1×10^{-3}	7.6

Table 6. Supercritical CO_2 Solubility of [RuCl(dfppp)(η-C_5H_5)] (**5**), [RuCl(dfppe)(η-C_5H_5)] (**6**), and [OsBr(dfppe)(η-C_5H_5)] (**8**)

compound	CO_2 density (g/mL)	pressure (bar)	temp. (°C)	concentration (mol/L)	concentration (g/L)
5	0.55	93	40	1.6×10^{-4}	0.3
5	0.60	97	40	5.8×10^{-4}	1.1
6	0.60	97	40	3.7×10^{-4}	0.7
8	0.60	97	40	3.0×10^{-4}	0.6

tells us that solute intermolecular forces need to be broken in order for the solute to dissolve.

With reference to using [$RuCl_2$(dfppp)$_2$] as a catalyst, its solubility of 1.1 g/L at a modest CO_2 density (0.6 g/mL) would be sufficiently high for catalytic activity. In Jessop's original production of DMF from CO_2, Me_2NH, and H_2, they generally used 3 μmol of catalyst for each reaction.[28] For the catalyst [$RuH_2(PMe_3)_4$] and a 50 mL reaction vessel, this equates to a 24 mg/L concentration, far below the solubility of our compounds. Another paper will highlight the catalytic testing of our complexes.

Conclusion

We have shown that it is possible to prepare highly fluorinated complexes of ruthenium and osmium by substituting the phosphine ligand aromatic groups with C_6F_{13} tails. This radically alters the solubility properties of the cyclopentadienyl complexes to the point where they become soluble in all organic solvents and only insoluble in water. However, the bis-diphosphine metal complexes when decorated with fluorous groups become insoluble in most organic solvents except diethylether. These complexes show enhanced solubility in supercritical carbon dioxide over the parent complexes, devoid of fluoro groups, and present the possibility for use as catalysts in this renewable solvent.

Acknowledgment. We thank the University of Western Australia for funding this project. B.M.B. was the holder of Australian Postgraduate Award.